

# Münsteranian Torturials on Nonlinear Science

edited by Uwe Thiele, Oliver Kamps, Svetlana Gurevich

## Continuation

# SITDROP: steady drop, hole and film states on a horizontal homogeneous substrate

Uwe Thiele<sup>1</sup>

Version 3, Jan 2022

For updates see [10.5281/zenodo.4546356](https://zenodo.org/record/4546356)

---

<sup>1</sup>with successive support of Christian Schelte, Frank Ehebrecht, Thomas Seidel, Simon Hartmann

### Abstract

The tutorial SITDROP is one of a series of tutorials on the practical application of numerical path-continuation methods for problems in soft matter and pattern formation. It is part of the “Münsterian Torturials on Nonlinear Science”. The tutorial explores an equation for steady drop- and hole-states derived from the dimensionless thin-film (or lubrication) equation. You will calculate steady solution of the equation by continuation in a number of different control parameters (domain size, liquid volume). The employed code package is `auto07p`.

## 1 Model

The tutorial SITDROP is part of the “Münsterian Torturials on Nonlinear Science”, a series of hands-on tutorials that shall facilitate the practical application of numerical path-continuation methods [1, 2, 3] for problems in soft matter and pattern formation by lowering the entrance threshold for systems where side conditions as, e.g., resulting from conservation laws and translational invariance, have to be taken into account. The present tutorial is based on the code package `auto07p` [4]. An overview of all available tutorials in the series and a description of a recommended sequence of working through them is given in Ref. [5].

The tutorial illustrates the calculation of steady drop and hole states of the dimensionless thin-film (or long-wave, or lubrication) equation [6, 7]. It is recommended to consider the tutorial in comparison to the tutorial ACCH [8] that investigates the mathematically similar (but simpler) Cahn-Hilliard equation [9].

The thin-film equation is an evolution equation for the height profile of a film or drop and is obtained by long-wave approximation from the Navier-Stokes equations and boundary conditions at the solid substrate and the free surface [6, 10, 11]. It reads

$$\partial_t h = -\partial_x \{Q(h) \partial_x [\partial_{xx} h - \partial_h f(h)]\} \quad (1)$$

where  $Q(h) = h^3$  is the mobility factor (not relevant for steady states). The equation can be written as a conserved gradient dynamics on an underlying energy functional similar to the Cahn-Hilliard equation [12, 7, 13]. In Eq. (1), the term in square brackets represents the negative of a pressure that consists of the Laplace (or curvature) pressure  $-\partial_{xx} h$  and an additional contribution  $\partial_h f(h)$  written as the derivative of a local free energy  $f(h)$ . The Laplace pressure is the pressure difference across a curved interface caused by its surface tension. Here, only the curvature of the free surface of the drop gives a contribution. In long-wave approximation it corresponds to the second spatial derivative of the height profile. For a sketch of the considered geometry see Fig. 1 (a).

The local free energy has a particular form for each studied problem. It may contain contributions due to wettability, hydrostatic pressure, electrostatic effects, or liquid-crystal elasticity. For specific examples see, e.g., [14, 15, 16, 17, 18]. In the tutorial we use a simple Derjaguin (or disjoining/conjoining) pressure  $\Pi(h) = -\partial_h f(h)$  that describes wettability for a partially wetting liquid (see reviews [19, 20, 21]). In particular, we employ the combination [16]

$$\partial_h f(h) = -\Pi(h) = \frac{1}{h^3} - \frac{1}{h^6}, \quad (2)$$

as shown in see Fig. 1 (b). To study steady states, i.e., resting droplets or films, we set  $\partial_t h = 0$  and integrate Eq. (1) twice. This is possible as the first integration constant, the flux  $C_0$ , is zero for systems without flow across the boundaries [10]. Then one may divide by the positive definite  $Q(h)$  and integrate a second time.

One obtains

$$0 = \partial_{xx}h(x) - \partial_h f(h) + C_1. \quad (3)$$

The constant  $C_1$  accounts for external conditions like chemical potential, vapor pressure or mass conservation. Here we consider the latter case where  $C_1$  takes the role of a Lagrange multiplier for mass conservation very similar to the role of  $\mu$  in the tutorial ACCH [8]. To use

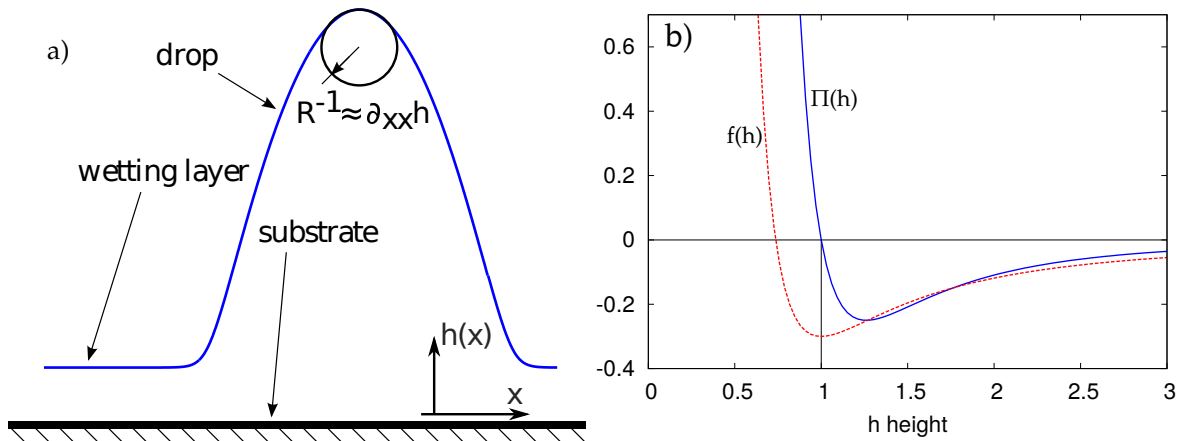


**Figure 1:** Panel (a) provides a sketch of the geometry employed in the tutorial SITDROP. It shows small droplet that coexists with an ultrathin adsorption or wetting layer (precursor film) in a situation with laterally periodic boundary conditions, as introduced in Eq. (6). Note that the radius of curvature can be both positive and negative and competes with the Derjaguin pressure  $\Pi(h)$ . Panel (b) gives typical functional dependencies of the wetting energy  $f(h)$  and  $\Pi(h) = -df/dh$ .

the continuation toolbox `auto07p` [4], we first write (3) as a system of first-order autonomous ordinary differential equations on the interval  $[0, 1]$ . Therefore, we introduce the variables  $u_1 = h - h_0$  and  $u_2 = dh/dx$ , and obtain from equation (3) the 2d dynamical system (NDIM = 2)

$$\begin{aligned} \dot{u}_1 &= Lu_2 \\ \dot{u}_2 &= L[f'(h_0 + u_1) - C_1]. \end{aligned} \quad (4)$$

where  $L$  is the physical domain size, and dots and primes denote derivatives with respect to  $\xi \equiv x/L$  and  $h$ , respectively. The advantage of the used form is that the fields  $u_1(\xi)$  and  $u_2(\xi)$  correspond to the correctly scaled physical fields  $h(L\xi)$  and  $\partial_x h(L\xi)$ . We use periodic boundary conditions for  $u_1$  and  $u_2$  (NBC = 2) that take the form

$$u_1(0) = u_1(1), \quad (5)$$

$$u_2(0) = u_2(1), \quad (6)$$

and two integral conditions (NINT = 2) that ensure (i) conservation of  $h$  and (ii) break the translation invariance of the states for the considered homogeneous substrate and the periodic BC. The integral condition for mass conservation (i) takes the form

$$\int_0^1 u_1 d\xi = 0. \quad (7)$$

As starting solution we use a small amplitude harmonic modulation of wavelength  $L_c = 2\pi/k_c$  where  $k_c = \sqrt{-f''_0}$  is the critical wavenumber for the linear instability of a flat film of thickness  $h_0$  and  $f''_0 = d^2 f/dh^2|_{h_0}$ . This results in  $C_1 = f'_0$  as starting value for  $C_1$  where  $f'_0 = df/dh|_{h_0}$ .

The number of free (continuation) parameters is given by  $NCONT = NBC + NINT - NDIM + 1$  and is here equal to 3.

As in the tutorial ACCH [8], there is a further complication as Eq. (4) corresponds to a conservative dynamical system (not a dissipative one). This can be seen when noting that Eq. (3) corresponds to Newton’s equation of motion when identifying  $x$  with time and  $h$  with position in Newton’s law. This implies that there is a hidden constant of motion - the energy - and trajectories in phase space are not attractors but form a dense one-parameter family of states. To deal with this one employs an “unfolding parameter”  $\epsilon$  that transforms the conservative into a “virtual” dissipative system (with the same solutions). Different formulations are possible. Here we use

$$\begin{aligned} \dot{u}_1 &= Lu_2 - \epsilon[f'(\bar{h} + u_1) - C_1] \\ \dot{u}_2 &= L[f'(\bar{h} + u_1) - C_1]. \end{aligned} \quad (8)$$

The technique is mentioned in the `auto07p` demo `r3b` [4] and further explained in Refs. [22, 23, 24]. It corresponds to the introduction of an unfolding term that embeds the conservative system into a one-parameter family of dissipative systems. Periodic solutions only exist for  $\epsilon = 0$ .

## 2 Runs

The diagram in Fig. 2 is determined through the continuation runs presented in the following table. The white fields describe what the individual runs do and mention important parameter settings including necessary changes. The grey fields give the `auto07` commands on the left when using the (modern) `Python` interface and on the right when using the more classic command line approach.

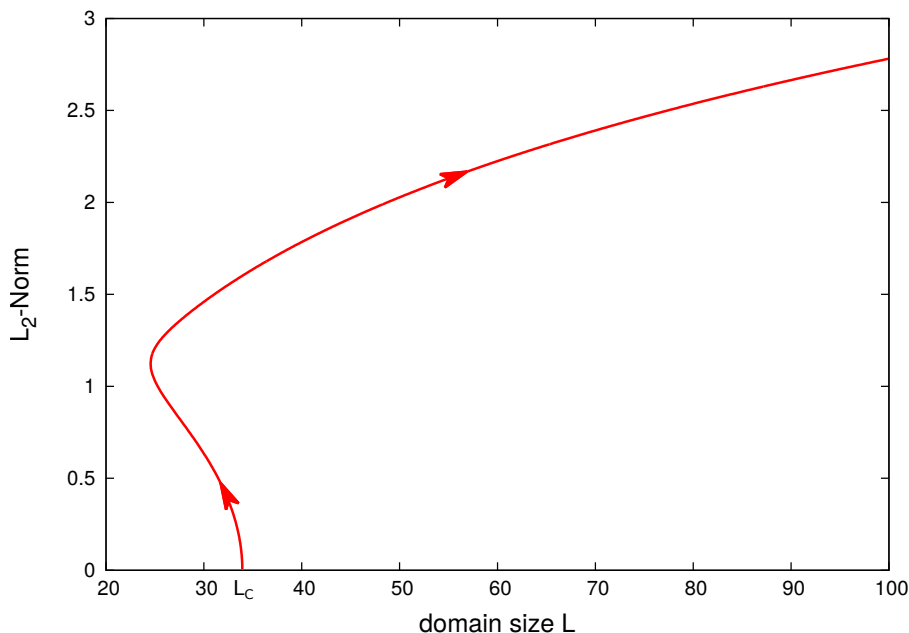


**Figure 2:** An illustration of the result of run 1 is given. The  $L_2$ -norm of steady states is shown in dependence of the main continuation parameter domain size  $L$  (PAR5) for a fixed mean film thickness  $h_0 = 3.0$ . The arrow indicates the direction of the path continuation.

Python interface command line	Terminal command line
<i>auto</i>	
<p><b>run 1:</b> Determine steady solutions as a function of domain size <math>L</math>, starting at the critical <math>L_c</math> with a small amplitude sinusoidal solution. Mean thickness <math>h_0 = 3</math> is fixed. One finds that the primary bifurcation is subcritical, and that the branch turns towards larger <math>L</math> at a saddle-node bifurcation at some <math>L_{sn} &lt; L_c</math>.</p> <p>Compute the branch of periodic solutions for <math>h_0 = 3</math> continued in <math>L</math> (PAR(5)) up to <math>L = 100</math>.</p> <p><b>Remaining true continuation parameters:</b> <math>C_1</math> (PAR(6)) and <math>\epsilon</math> (PAR(2));</p> <p><b>Other output:</b> amplitude of <math>h</math> (PAR(7)), maximal slope of <math>h</math>. i.e., the mesoscopic contact angle <math>\theta_{mes}</math> (PAR(46))</p> <p><b>Parameter:</b> IPS= 4, ISP= 0, ISW= 1, ICP= [5, 6, 2, 7, 46],</p> <p>Start data from function <i>stpnt</i> (IRS= 0)</p> <p>save output-files as <i>b.d1</i>, <i>s.d1</i>, <i>d.d1</i></p>	
<i>r1 = run(e = 'sitdrop', c = 'sitdrop.1', sv = 'd1')</i>	<i>@@R sitdrop 1</i> <i>@sv d1</i>
<p><b>run 11:</b> Restart at domain size <math>L = 100</math>, change mean thickness <math>h_0</math>.</p> <p>Continued in mean thickness <math>h_0</math> (PAR(1)) for fixed domain size <math>L</math>. Stop at <math>h_0 = 10</math></p> <p><b>Remaining true continuation parameters:</b> <math>C_1</math> (PAR(6)) and <math>\epsilon</math> (PAR(2))</p> <p><b>Other output:</b> as in run 1</p> <p><b>Parameters:</b> IPS= 4, ISP= 0, ISW= 1, ICP= [1, 6, 2, 7, 46],</p> <p>Start at final result of run 1: IRS= 7</p> <p>save output-files as <i>b.d11</i>, <i>s.d11</i>, <i>d.d11</i></p>	
<i>r11 = run(r1, e = 'sitdrop', c = 'sitdrop.11', sv = 'd11')</i>	<i>@@R sitdrop 11 d1</i> <i>@sv d11</i>
<p><b>run 2:</b> Same as run 1 but continuing to large drops <math>L = 10^5</math>.</p> <p>save output-files as <i>b.d2</i>, <i>s.d2</i>, <i>d.d2</i></p>	
<i>r2 = run(e = 'sitdrop', c = 'sitdrop.2', sv = 'd2')</i>	<i>@@R sitdrop 2</i> <i>@sv d2</i>
Plot the results.	
<i>plot('d1')</i> <i>plot('d11')</i> <i>plot('d2')</i>	<i>@pp d1</i> <i>@pp d11</i> <i>@pp d2</i>
<i>clean()</i>	<i>@cl</i>

Table 1: Commands for running tutorial SITDROP.

### 3 Remarks:

- In context of a nonconserved dynamics, i.e., allowing for evaporation/condensation, the constant  $C_1$  corresponds to the negative of a chemical potential or partial vapour pressure.
- The *f90* file provides as FI(3) another integral condition that has up to here not been used in the tutorial. When switched on by setting NINT to 3 in the *c.* file and adding PAR9 at the end list of true continuation parameters within the array in ICP it determines the

energy per length of the obtained states. This facilitates the interpretation of the physical meaning of the found states.

- Beside the NCONT true continuation parameters that have to be given as ICP in the `c.*` parameter file, one may list other output parameters as defined in the subroutine PVLS in the `*.f90` file, for instance, the amplitude PAR7 or the steepest slope PAR46. The latter corresponds to the slope at the inflection point and is often used as an approximation of the equilibrium contact angle.
- The command line commands and the resulting screen output are also provided in the accompanying README file.

## 4 Tasks:

After running the examples, try to implement your own adaptations, e.g.:

1. Redo run 1 for other values of the mean height  $h_0$ , e.g., 1.27, 1.5, 2.5, 5.0, 10.0. What do you observe? Typical results are given in Fig. 3.
2. Redo run 11 allowing the code to go beyond  $h_0 = 10$ . What do you observe? Typical results are given in Fig. 4.
3. Run a continuation at fixed  $C_1$  (you need to “set free” some other parameter). Compare your results with [7]. Typical results are given in Fig. 5.
4. Activate the additional integral condition to measure the energy

$$E = \int_L \left[ \frac{u_2^2}{2} + f(h) - f(h_0) \right] d\xi \quad (9)$$

of the solutions. Typical results are given in Fig. 6.

5. Replace the used Derjaguin pressure by a different one that you get from the literature. ([17], [25] or [14])

## 5 Outlook

Building on the here presented application of continuation techniques to thin-film equations to determine steady sitting drops on homogeneous substrates many other situations may be investigated. From there, you may advance either to the linear stability of these states with the tutorial LINDROP [26], or to drops on a heterogeneous substrate with the tutorial HETDROP [27], or to sliding drops on an incline with the tutorial SLIDROP [28]. Finally, tutorials HETDRIV [29] and ROTFFTW [30] combine aspects of the latter two, investigating steady droplets on a heterogeneous inclined substrate and their stick-slipping motion beyond depinning. Furthermore, tutorial DRIST [31] determines the linear stability of sliding drops by continuing the corresponding states, their eigenvalues and eigenfunctions in parameter space. This includes the determination of transversal instabilities of sliding liquid ridges.

Similar concepts can be applied for related thin-film problems. In the literature one finds examples of the continuation of self-similar states occurring during film rupture [32, 33], the continuation of square and hexagon patterns of drops on 2d substrates (see [34] and section 3.2 of [35]), as well as the continuation of drop states for two-layer systems or on elastic substrates [36, 37].

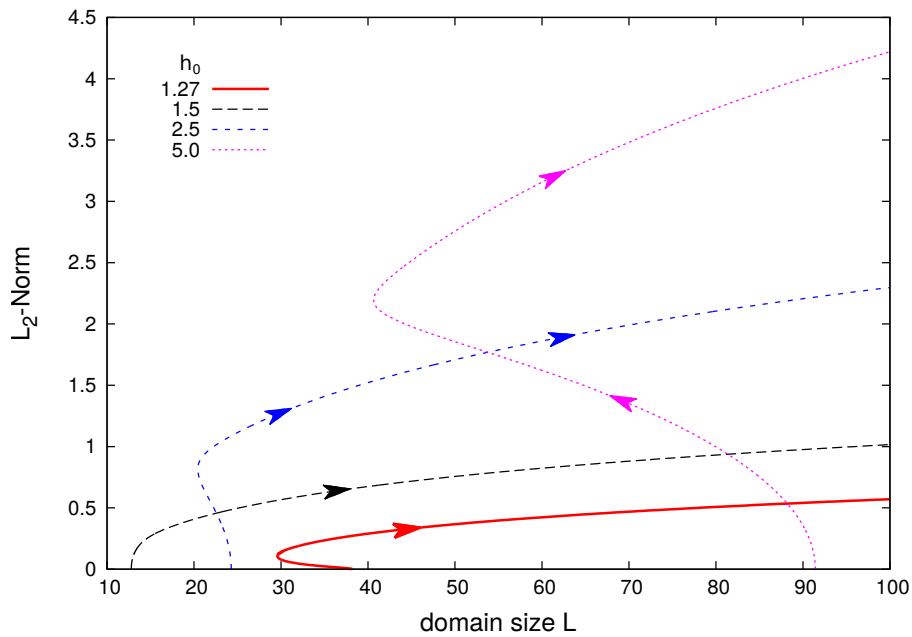


**Figure 3:** An illustration for task 1 is given. The  $L_2$ -norm of steady states is shown in dependence of the main continuation parameter domain size  $L$  (PAR5) for various fixed mean film thicknesses as given in the legend.

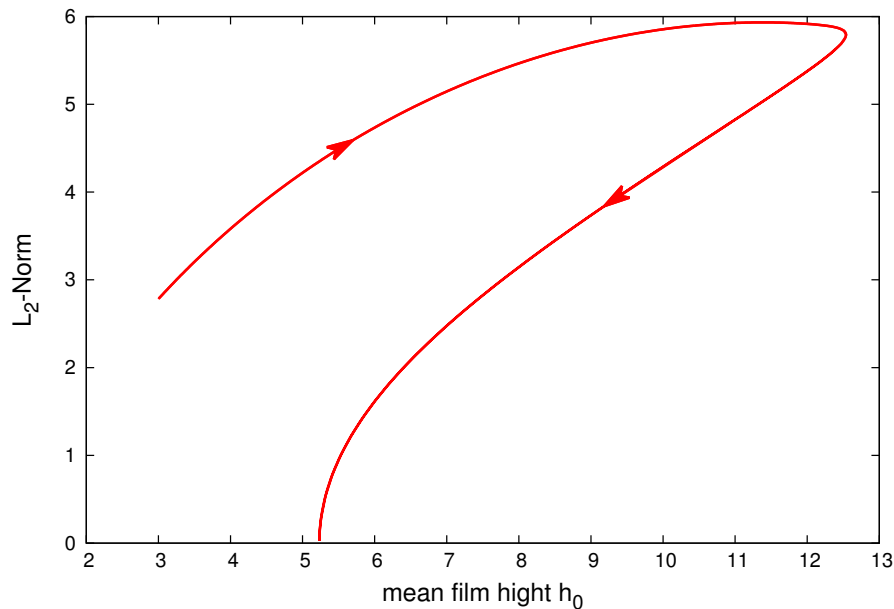


**Figure 4:** An illustration for task 2 is given. The  $L_2$ -norm is shown in dependence of the mean film height  $h_0$  (PAR1) for fixed domain size  $L = 100$ . The drop size increases with  $h_0$  up to  $h_0 \approx 12.5$  where a saddle-node bifurcation occurs (the drop fills the entire domain). The lower branch corresponds to unstable hole (nucleation) solutions. The arrow indicates the direction of the path continuation run.

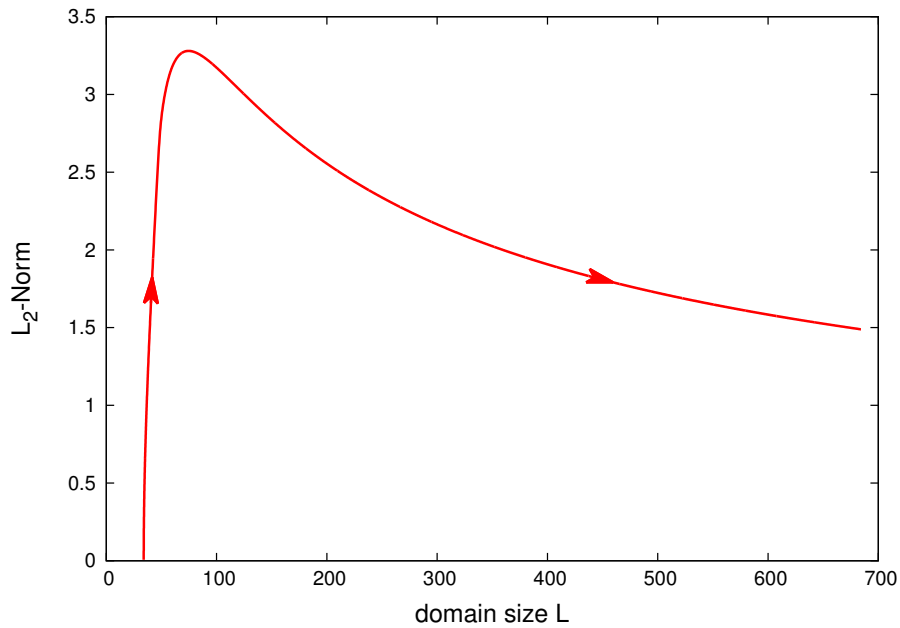


**Figure 5:** An illustration for task 3 is given. The  $L_2$ -norm is shown in dependence of domain size  $L$  (PAR5) for fixed chemical potential  $C_1 = df/dh|_{h=h_0=3}$  (PAR6). Now the primary bifurcation is supercritical in contrast to the case of Fig. 2.

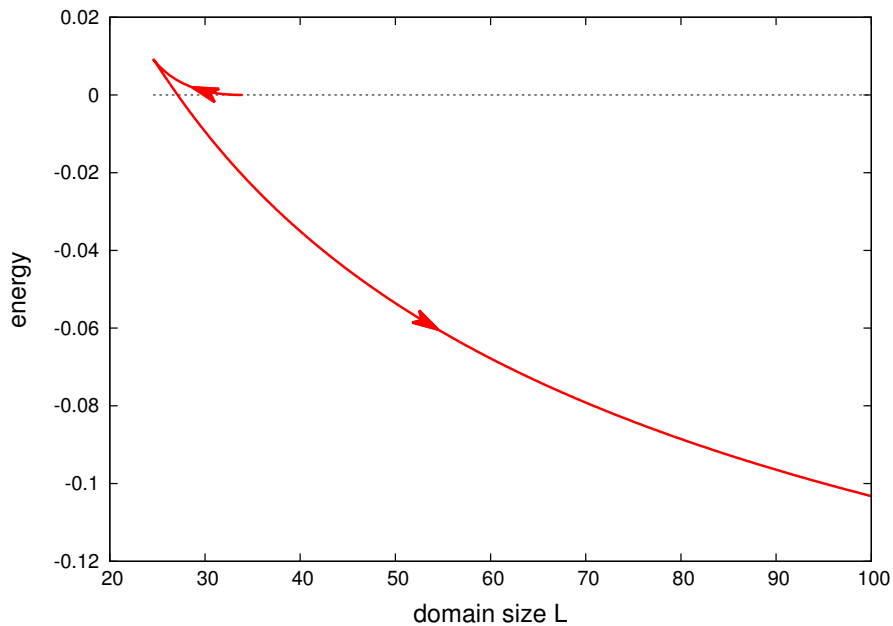


**Figure 6:** An illustration for task 4 is given. The energy (9) is shown in dependence of domain size  $L$  (PAR5) for fixed mean film thickness  $h_o = 3.0$ .

## References

- [1] E. Doedel, H. B. Keller, and J. P. Kernevez. “Numerical analysis and control of bifurcation problems (I) Bifurcation in finite dimensions”. In: *Int. J. Bifurcation Chaos* 1 (1991), pp. 493–520. DOI: [10.1142/S0218127491000397](https://doi.org/10.1142/S0218127491000397).
- [2] B. Krauskopf, H. M. Osinga, and J Galan-Vioque, eds. *Numerical Continuation Methods for Dynamical Systems*. Dordrecht: Springer, 2007. DOI: [10.1007/978-1-4020-6356-5](https://doi.org/10.1007/978-1-4020-6356-5).
- [3] H. A. Dijkstra et al. “Numerical bifurcation methods and their application to fluid dynamics: Analysis beyond simulation”. In: *Commun. Comput. Phys.* 15 (2014), pp. 1–45. DOI: [10.4208/cicp.240912.180613a](https://doi.org/10.4208/cicp.240912.180613a).
- [4] E. J. Doedel and B. E. Oldeman. *AUTO07p: Continuation and bifurcation software for ordinary differential equations*. Montreal: Concordia University, 2009. URL: <http://indy.cs.concordia.ca/auto>.
- [5] U. Thiele. *Münsterian Torturials on Nonlinear Science: Overview of available tutorials on path continuation*. Ed. by U. Thiele, O. Kamps, and S. V. Gurevich. 2021. DOI: [10.5281/zenodo.4548111](https://doi.org/10.5281/zenodo.4548111).
- [6] A. Oron, S. H. Davis, and S. G. Bankoff. “Long-scale evolution of thin liquid films”. In: *Rev. Mod. Phys.* 69 (1997), pp. 931–980. DOI: [10.1103/RevModPhys.69.931](https://doi.org/10.1103/RevModPhys.69.931).
- [7] U. Thiele. “Thin film evolution equations from (evaporating) dewetting liquid layers to epitaxial growth”. In: *J. Phys.: Condens. Matter* 22 (2010), p. 084019. DOI: [10.1088/0953-8984/22/8/084019](https://doi.org/10.1088/0953-8984/22/8/084019).
- [8] U. Thiele. *Münsterian Torturials on Nonlinear Science: ACCH - steady states of Allen-Cahn and Cahn-Hilliard equations*. Ed. by U. Thiele, O. Kamps, and S. V. Gurevich. 2021. DOI: [10.5281/zenodo.4545409](https://doi.org/10.5281/zenodo.4545409).
- [9] Uwe Thiele. *Lecture “Cahn-Hilliard-type phase-transition dynamics”, WWU Münster, Winter Term 2020/21*. Video and Slides on zenodo. 2021. DOI: [10.5281/zenodo.4545361](https://doi.org/10.5281/zenodo.4545361). (Visited on 02/17/2021).
- [10] U. Thiele. “Structure formation in thin liquid films”. In: *Thin Films of Soft Matter*. Ed. by S. Kalliadasis and U. Thiele. Vienna: Springer Vienna, 2007, pp. 25–93. ISBN: 978-3-211-69808-2. DOI: [10.1007/978-3-211-69808-2\\_2](https://doi.org/10.1007/978-3-211-69808-2_2).
- [11] R. V. Craster and O. K. Matar. “Dynamics and stability of thin liquid films”. In: *Rev. Mod. Phys.* 81 (2009), pp. 1131–1198. DOI: [10.1103/RevModPhys.81.1131](https://doi.org/10.1103/RevModPhys.81.1131).
- [12] V. S. Mitlin. “Dewetting of solid surface: Analogy with spinodal decomposition”. In: *J. Colloid Interface Sci.* 156 (1993), pp. 491–497. DOI: [10.1006/jcis.1993.1142](https://doi.org/10.1006/jcis.1993.1142).
- [13] U. Thiele. “Recent advances in and future challenges for mesoscopic hydrodynamic modelling of complex wetting”. In: *Colloids Surf. A* 553 (2018), pp. 487–495. DOI: [10.1016/j.colsurfa.2018.05.049](https://doi.org/10.1016/j.colsurfa.2018.05.049).
- [14] A. Sharma. “Equilibrium contact angles and film thicknesses in the apolar and polar systems: Role of intermolecular interactions in coexistence of drops with thin films”. In: *Langmuir* 9 (1993), p. 3580. DOI: [10.1021/1a00036a038](https://doi.org/10.1021/1a00036a038).
- [15] G. F. Teletzke, H. T. Davis, and L. E. Scriven. “Wetting hydrodynamics”. In: *Rev. Phys. Appl. (Paris)* 23 (1988), pp. 989–1007. DOI: [10.1051/rphysap:01988002306098900](https://doi.org/10.1051/rphysap:01988002306098900).
- [16] L. M. Pismen. “Nonlocal diffuse interface theory of thin films and the moving contact line”. In: *Phys. Rev. E* 64 (2001), p. 021603. DOI: [10.1103/PhysRevE.64.021603](https://doi.org/10.1103/PhysRevE.64.021603).

- [17] U. Thiele, M. G. Velarde, and K. Neuffer. “Dewetting: Film rupture by nucleation in the spinodal regime”. In: *Phys. Rev. Lett.* 87 (2001), p. 016104. DOI: [10.1103/PhysRevLett.87.016104](https://doi.org/10.1103/PhysRevLett.87.016104).
- [18] U. Thiele et al. “Film rupture in the diffuse interface model coupled to hydrodynamics”. In: *Phys. Rev. E* 64 (2001), p. 031602. DOI: [10.1103/PhysRevE.64.031602](https://doi.org/10.1103/PhysRevE.64.031602).
- [19] V. M. Starov and M. G. Velarde. “Surface forces and wetting phenomena”. In: *J. Phys.-Condens. Matter* 21 (2009), p. 464121. DOI: [10.1088/0953-8984/21/46/464121](https://doi.org/10.1088/0953-8984/21/46/464121).
- [20] P.-G. de Gennes. “Wetting: Statics and dynamics”. In: *Rev. Mod. Phys.* 57 (1985), pp. 827–863. DOI: [10.1103/RevModPhys.57.827](https://doi.org/10.1103/RevModPhys.57.827).
- [21] D. Bonn et al. “Wetting and spreading”. In: *Rev. Mod. Phys.* 81 (2009), pp. 739–805. DOI: [10.1103/RevModPhys.81.739](https://doi.org/10.1103/RevModPhys.81.739).
- [22] E. J. Doedel et al. “Computation of periodic solutions of conservative systems with application to the 3-body problem”. In: *Int. J. Bifurcation Chaos* 13 (2003), pp. 1353–1381. DOI: [10.1142/S0218127403007291](https://doi.org/10.1142/S0218127403007291).
- [23] F. J. Munoz-Almaraz et al. “Continuation of periodic orbits in conservative and Hamiltonian systems”. In: *Physica D* 181 (2003), pp. 1–38. DOI: [10.1016/S0167-2789\(03\)00097-6](https://doi.org/10.1016/S0167-2789(03)00097-6).
- [24] F. J. Munoz-Almaraz et al. “Continuation of normal doubly symmetric orbits in conservative reversible systems”. In: *Celest. Mech. Dyn. Astron.* 97 (2007), pp. 17–47. DOI: [10.1007/s10569-006-9048-3](https://doi.org/10.1007/s10569-006-9048-3).
- [25] A. Sharma. “Relationship of thin film stability and morphology to macroscopic parameters of wetting in the apolar and polar systems”. In: *Langmuir* 9 (1993), pp. 861–869. DOI: [10.1021/la00027a042](https://doi.org/10.1021/la00027a042).
- [26] U. Thiele. *Münsterian Torturials on Nonlinear Science: LINDROP - linear stability of steady states on a horizontal homogeneous substrate*. Ed. by U. Thiele, O. Kamps, and S. V. Gurevich. 2021. DOI: [10.5281/zenodo.4546375](https://doi.org/10.5281/zenodo.4546375).
- [27] U. Thiele. *Münsterian Torturials on Nonlinear Science: HETDROP - steady drop and film states on a horizontal heterogeneous substrate*. Ed. by U. Thiele, O. Kamps, and S. V. Gurevich. 2021. DOI: [10.5281/zenodo.4546377](https://doi.org/10.5281/zenodo.4546377).
- [28] U. Thiele. *Münsterian Torturials on Nonlinear Science: SLIDROP - sliding drops on an inclined homogeneous substrate*. Ed. by U. Thiele, O. Kamps, and S. V. Gurevich. 2021. DOI: [10.5281/zenodo.4546381](https://doi.org/10.5281/zenodo.4546381).
- [29] U. Thiele. *Münsterian Torturials on Nonlinear Science: HETDRIV - steady drops on a heterogeneous substrate under lateral driving*. Ed. by U. Thiele, O. Kamps, and S. V. Gurevich. 2021. DOI: [10.5281/zenodo.4546379](https://doi.org/10.5281/zenodo.4546379).
- [30] U. Thiele. *Münsterian Torturials on Nonlinear Science: ROTFFTW - steady and time-periodic drops on a rotating cylinder*. Ed. by U. Thiele, O. Kamps, and S. V. Gurevich. 2021. DOI: [10.5281/zenodo.4546383](https://doi.org/10.5281/zenodo.4546383).
- [31] U. Thiele. *Münsterian Torturials on Nonlinear Science: DRIST - linear stability of sliding drops on an inclined homogeneous substrate*. Ed. by U. Thiele, O. Kamps, and S. V. Gurevich. 2021. DOI: [10.5281/zenodo.4546407](https://doi.org/10.5281/zenodo.4546407).
- [32] D. Tseluiko, J. Baxter, and U. Thiele. “A homotopy continuation approach for analysing finite-time singularities in thin liquid films”. In: *IMA J. Appl. Math.* 78 (2013), pp. 762–776. DOI: [10.1093/imamat/hxt021](https://doi.org/10.1093/imamat/hxt021).

- [33] M. C. Dallaston et al. “Self-similar finite-time singularity formation in degenerate parabolic equations arising in thin-film flows”. In: *Nonlinearity* 30 (2017), pp. 2647–2666. DOI: [10.1088/1361-6544/aa6eb3](https://doi.org/10.1088/1361-6544/aa6eb3).
- [34] P. Beltrame and U. Thiele. “Time integration and steady-state continuation method for lubrication equations”. In: *SIAM J. Appl. Dyn. Syst.* 9 (2010), pp. 484–518. DOI: [10.1137/080718619](https://doi.org/10.1137/080718619).
- [35] Sebastian Engelnkemper. “Nonlinear Analysis of Physicochemically Driven Dewetting - Statics and Dynamics”. PhD thesis. Münster: Westfälische Wilhelms-Universität Münster, 2017.
- [36] A. Pototsky et al. “Morphology changes in the evolution of liquid two-layer films”. In: *J. Chem. Phys.* 122 (2005), p. 224711. DOI: [10.1063/1.1927512](https://doi.org/10.1063/1.1927512).
- [37] C. Henkel, J. H. Snoeijer, and U. Thiele. “Gradient-dynamics model for liquid drops on elastic substrates”. In: *Soft Matter* 17 (2021). Corresponding data can be found on zenodo under <http://doi.org/10.5281/zenodo.5607074>, pp. 10359–10375. DOI: [10.1039/D1SM01032H](https://doi.org/10.1039/D1SM01032H).